Thickness Effect on the Optical Parameters of Ge-Se-Te Films

A. M. Bakry and A. El-Korashy[+]

Physics Department, Faculty of Science, Ain-Shams University, Cairo, Egypt 11566.
(+) Dr. Sorour Res. Lab., Physics Dept., Faculty of science, Assiut University, Assiut, Egypt.
E-mail: assem_sedfy@asunet.shams.edu.eg

Thin films of $Ge_{30}Se_{50}Te_{20}$ with thickness of 100, 150, 200 and 250 nm were prepared by thermal evaporation technique on glass substrates. Normal-incidence optical transmission spectra have been measured in the range from 190 to 900 nm. The optical constants were calculated using Swanepoel's method. The effect of film thickness on the optical constants had been investigated. Analysis of the refractive index (n) yields the values of the high frequency dielectric constant (ε_∞), Wemple's single oscillator energy E_w, dispersion energy E_d, the oscillator wavelength (λ_o), the average oscillator strength (S_o) and carrier concentration N/m^* at different thickness. Optical absorption measurements showed that fundamental absorption edge is a function of the film thickness. The optical gap energy E_g is determined. The variation of the optical constants with film thickness was reported. The results are interpreted on the basis of the local field correction theory.

1. Introduction

Chalcogenide glasses have attracted much attention due to their wide technological applications [1], such as: IR detector [2], electronic and optical switches [3, 4], inorganic resist [5] and optical recording media [6]. Chalcogenide glasses have also applications as electronic and optoelectronic device materials [7]. The materials containing a chalcogen element is widely used in switching and memory devices [8, 9].

The optical properties of chalcogenide glasses have been the subject of many recent papers [10, 11]. The optical characterization of thin films, i.e., measurements of refractive index *n*, extinction coefficient *k* and optical gap E_g, requires accurate measurements of both optical transmission and/or reflection spectra. The optical constants, using only the transmission spectra, could be calculated using a method proposed by Swanepoel [12] which is independent

on film-thickness uniformity. This method is based on the upper and lower envelopes of normal-incidence optical transmission spectra.

Studies for the dependence of optical parameters on film thickness for chalcogenide glasses have been reported by various researchers [13-28]. Unfortunately not much was reported for this kind of study on GeSeTe system[13].

The aim of the present work: first, to calculate the optical constants of Ge-Se-Te thin films by the envelope method, proposed by Swanepoel [12]. Second, to study the effect of the film thickness on the optical constants of $Ge_{30}Se_{50}Te_{20}$ thin films.

2. Experimental

Bulk glasses of $Ge_{30}Se_{50}Te_{20}$ system were prepared by the conventional melt-quenching technique. High purity (99.999% pure) Ge, Se and Te in appropriate atomic percentage proportions were weighed and placed in quartz ampoules. The contents of the ampoules were sealed in a vacuum of 10^{-4} torr and then placed in automated Muffle Furnace where the temperature was increased at the rate of 3 K/min up to 1373 K and kept at that temperature for 24 h. Quenching was carried out into ice water mixture to obtain the glassy nature.

Amorphous $Ge_{30}Se_{50}Te_{20}$ films were prepared by thermal evaporation under vacuum of 10^{-5} torr. Films were deposited on ultrasonically cleaned Corning 7059 glass slides. The optical transmittance and reflectance spectra were obtained using a computerized SHIMADZU UV-2100 double beam spectro-phototometer. The measurements were carried out in the wavelength range 190 - 900 nm. The relative uncertainty in the transmittance and reflectance given by the manufacturer is 0.2%. Transmittance scans were performed using a glass substrate in the reference compartment of the same kind as the one used for the film.

3. Results and discussion:

Optical constants are deduced from the fringes pattern in the transmittance spectrum. According to Swanepoel [12], the value of the refractive index of the film can be calculated by using the following expression (the error in calculating the refractive index n using this method is ≈ 0.001): in the transparent region where the absorption coefficient $\alpha \approx 0$, the refractive index (n) is given by

$$n = [N + (N^2 - s^2)^{1/2}]^{1/2} \quad \text{.....................(1)}$$

where

$$N = \frac{2s}{T_m} - \frac{(s^2 + 1)}{2} \quad \text{..................................(2)}$$

T_m is the envelope function of minimum transmittance and s is the refractive index of the substrate (s = 1.52).

In the weak absorption region where $\alpha \neq 0$ the transmittance decreases due to the influence of α and equation (2) becomes

$$N = 2s\frac{T_M - T_m}{T_M T_m} + \frac{s^2 + 1}{2} \quad \text{...........................(3)}$$

where T_M is the envelope function of maximum transmittance. The refractive index can be estimated by extrapolating envelopes corresponding to T_M and T_m.

In the region of strong absorption, n values are calculated by extrapolating the values calculated in the other parts of the spectrum using the classical Cauchy expression:

$$n = \frac{a}{\lambda^2} + b \quad \text{..(4)}$$

where a and b are material dependent constants.

The film thickness d was calculated using the basic equation for interference fringes [12]. Suppose the order number (integer or half integer) of the first extreme is m_1. Then

$$2nd = (m_1 + \frac{l}{2})\lambda \quad \text{..................................(5)}$$

where l = 0, 1, 2, 3,…….

$$\frac{l}{2} = 2d(\frac{n}{\lambda}) - m_1 \quad \text{....................................(6)}$$

Plotting $l/2$ against n/λ yields a straight line with a slope = $2d$ and intercept with the vertical axis = $-m_1$.

The extinction coefficient is a measure of the fraction of light lost due to scattering and absorption per unit distance of the participating medium. The extinction coefficient *k* has been calculated using the relation

$$k = \frac{\alpha\lambda}{4\pi} \quad \text{...(7)}$$

where α is the absorption coefficient which is given by

$$\alpha = (\frac{1}{d})\ln(\frac{1}{x}) \quad \text{..(8)}$$

where x is the absorbance [12].

Figure (1) shows the variation of the absorption coefficient versus photon energy. From the figure it could seen that the absorption coefficient decreases with increasing in film thickness and the absorption edge shifts to lower values of energy with increase in film thickness. The same behavior was previously reported for FeS_2 for thickness ≥ 130 nm [26], for InSe films having thickness > 80 nm [23], for $(Ge_2S_3)_1(Sb_2Se_3)_1$ [25] and for $Se_{85}Te_{15}$ films [27]. This was attributed to an increased proportion of bulk defects in thicker films [26] and to a low transition probability of carriers [23]. Fig. (1) also reveals that for a thickness greater than 200 nm, the absorption coefficient decreases in the absorption edge region.

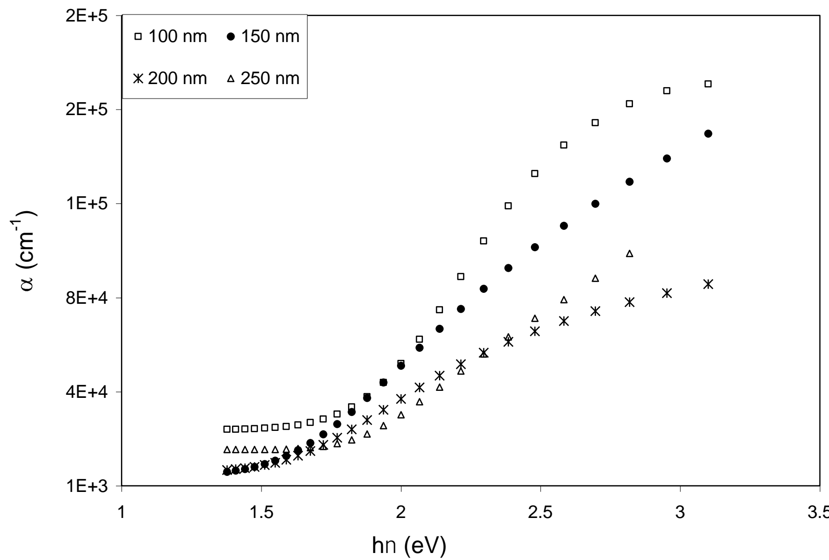

Fig. (1): the absorption coefficient α vs. photon energy ($h\nu$) of amorphous $Ge_{30}Se_{50}Te_{20}$ films at different thickness.

The optical absorption spectrum is found to have three distinct regions [29]: the region of weak absorption tail which originates from defects and impurities, the exponential region which is strongly related to the structural randomness of the system and the high absorption region which determines the optical energy gap. In the last region, the following parabolic relation could be applied :

$$\alpha h\nu = B\left(h\upsilon - E_g\right)^r \quad \ldots\ldots\ldots\ldots\ldots\ldots\ldots\ldots\ldots\ldots(9)$$

where B is a constant which depends on the transition probability, E_g is the optical gap energy and r is an index which can be assumed to have values of 1/2 and 2 depending on the nature of the electronic transition responsible for the absorption. r = 1/2 for allowed direct transition and r = 2 for allowed indirect transition [30].

The experimental results of α versus $h\nu$ were fitted to eq. (9) by the least-squares method. The results for the amorphous $Ge_{30}Se_{50}Te_{20}$ films at different thickness showed a best fit to eq (9) with r = 2 and r = ½ indicated that there exist both types of transitions, direct and indirect one. The optical band gap (E_g) of the direct and indirect transitions can be obtained from the intercept of the $(\alpha h\nu)^r$ vs. $h\nu$ plots with the energy axis at $(\alpha h\nu)^r = 0$ as shown in Figs. (2) and (3). A list of the calculated values for energy gaps is given in table (1). The experimental results show that the optical energy gap decreases as the film thickness increases from 100 to 200 nm. Similar results were previously reported for the same structure with different composition values [13] due to unsaturated bonds, for CdSe [14, 16] CdS [20] and $CuInSe_2$ [21] due to increase in particle size and decrease in strain and dislocation energy, CdSnSe [17, 18] due to quantum size effect, FeS_2 [26] for thickness ≥ 130 nm due to grain boundaries forming defect states in the forbidden zones of energy band and AsGeSe [28]. It is worth noting that although the above studies were done on different thickness ranges they came up with same conclusion. For the 250 nm thickness, E_g increased. This increase is confirmed with the behavior of the α graph, shown in Fig. (1), for this thickness.

For many amorphous materials, in the exponential region of absorption (second region), α obeys Urbach's empirical relation [31]:

$$\alpha = \alpha_o \exp(h\nu / E_u) \quad \ldots\ldots\ldots\ldots\ldots\ldots\ldots\ldots\ldots(10)$$

where α_o is a constant, h is Planck's constant and E_u is an energy which is often interpreted as the width of the tails of the localized states in the band gap region. Tauc [32] believes that it arises from electronic transitions between localized states in the band edge tails, the density of which is assume to fall exponentially with energy.

A plot of $\ln\alpha$ as a function of the photon energy for $Ge_{30}Se_{50}Te_{20}$ for different film thickness is shown in Fig.(4). The calculated values of E_u are listed in Table (1). From the table it could be seen that the width of Urbach tail increases with increasing the film thickness from 100 to 200 nm. For thickness > 200, E_u decreased. The same behavior was previously observed for $As_{25}Ge_{45}Se_{30}$ for thickness > 200 nm [28]. The trend shown for E_u was expected since it represents the opposite to that for E_g.

The refractive index of the prepared $Ge_{30}Se_{50}Te_{20}$ films calculated using eq. (1) is shown in Fig. (5). It is clear from the figure that the refractive index curves shift to higher values with increase in thickness. The same conclusion was drawn for a previous study conducted on the same composition [13]. But for a different composition (GeSe), n behaved oppositely. Also for CdSe [14], for AsTeIn (for thickness < 800 nm) and was attributed to the discontinuity of the film in the initial stages of deposition [15], for $CuInSe_2$ [21] and SeTe [27] due to dependence on the internal microstructure induced by the film thickness.

Table (1): Values of refractive index n, real and imaginary parts of dielectric constant ε_r and ε_i, respectively, at $\lambda = 600$ nm. The high-frequency dielectric constant ε_∞, Tauc energy gap E_g, Urbach parameter E_u, Wemple single oscillator energy (average gap) E_w and dispersion energy E_d, the oscillator wavelength λ_o, the average oscillator strength S_o and carrier concentration N/m^* at different thickness.

Thickness	n	ε_r	ε_i	ε_∞	E_g Direct	E_g Indirect	E_u	E_w	E_d	S_o 10^{-5}	λ_o	N/m^* 10^{20}
100	2.68	7.11	1.62	5.7	2.07	1.34	0.37	2.533	5.299	2.41	155.26	8.05
150	4.16	17.22	2.37	7.3	2.03	1.25	0.43	2.247	5.748	2.79	528.20	5.46
200	5.31	28.16	2.17	7.6	1.98	1.15	0.49	2.101	5.414	2.97	545.06	4.84
250	5.67	32.14	1.99	7.2	2.11	1.32	0.42	2.128	5.527	3.10	556.85	1.8

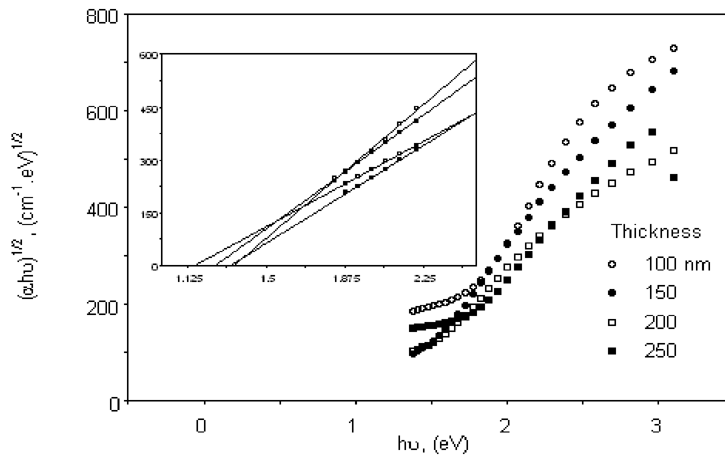

Fig. (2): $(\alpha h\nu)^{1/2}$ vs. photon energy $(h\nu)$ of amorphous $Ge_{30}Se_{50}Te_{20}$ films at different thickness

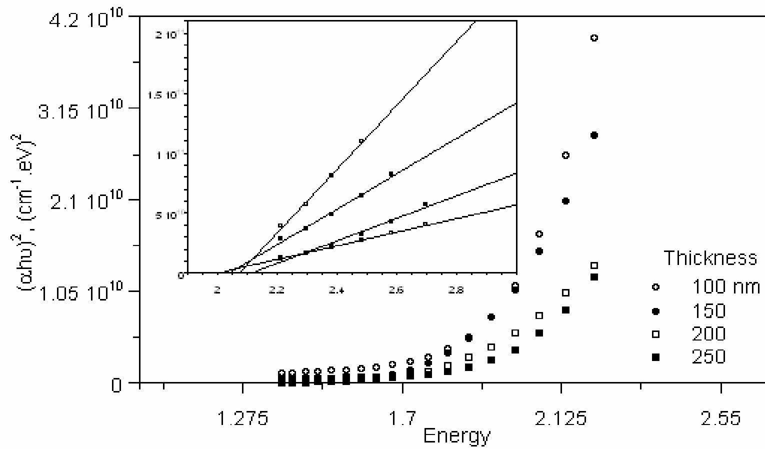

Fig. (3): $(\alpha h\nu)^2$ vs. photon energy (hν) of amorphous $Ge_{30}Se_{50}Te_{20}$ films at different thickness

The complex dielectric constant is a fundamental intrinsic material property. The real part of the dielectric constant is associated with the term that shows how much it will slow down the speed of light in the material and the imaginary part shows how a dielectric absorbs energy from an electric field due to dipole motion. The real and imaginary parts of the dielectric constant were determined using the relations derived from the complex refractive index [33]:

$$\varepsilon_r = n^2 - k^2 \qquad (11)$$

and

$$\varepsilon_i = 2nk \qquad (12)$$

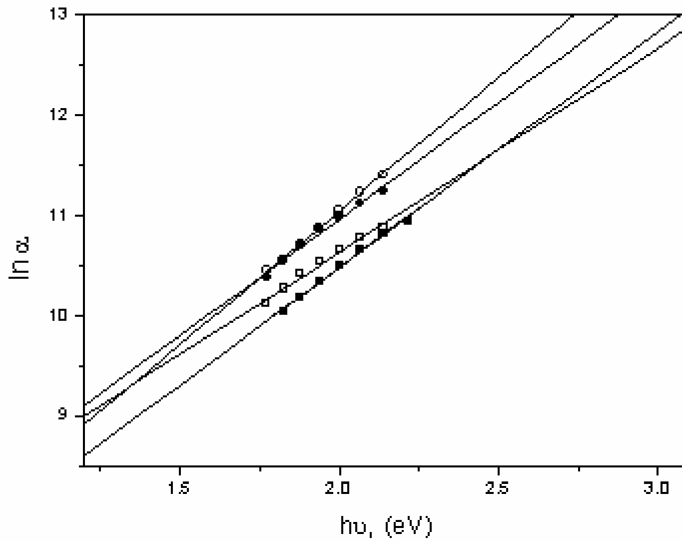

Fig. (4): lnα vs. photon energy (hv) of amorphous $Ge_{30}Se_{50}Te_{20}$ films at different thickness

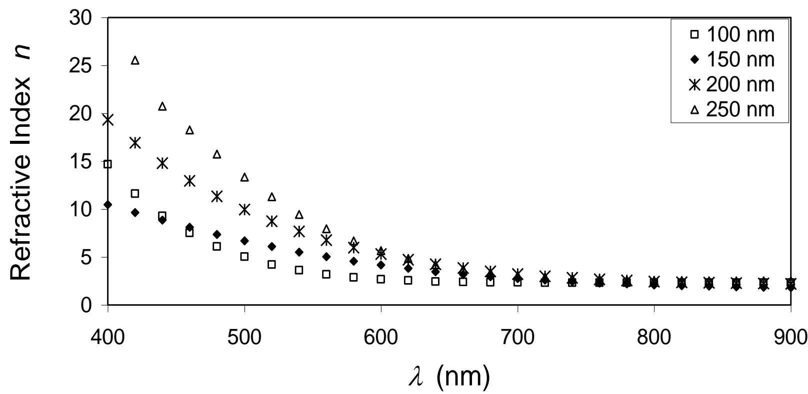

Fig. (5): The relation between the refractive (n) index and the wavelength for amorphous $Ge_{30}Se_{50}Te_{20}$ films.

The variation of both the real and imaginary parts of the dielectric constant ε_r and ε_i for $Ge_{30}Se_{50}Te_{20}$ films are illustrated in Figs. (6) and (7). Their values at wavelength 600 nm are listed in the table 1. It is clear from the table that the value of ε_r increases with thickness while ε_i value increased at thickness range 100 – 150 nm and then started to decrease.

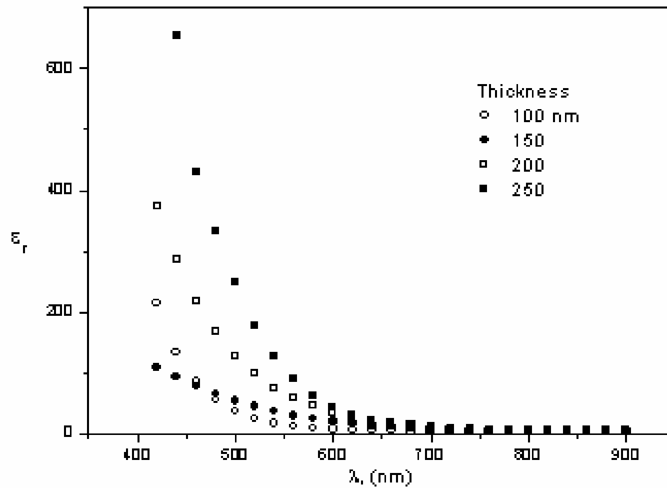

Fig. (6): The relation between the real part of the dielectric constant (ε_r) and the wavelength for $Ge_{30}Se_{50}Te_{20}$ films.

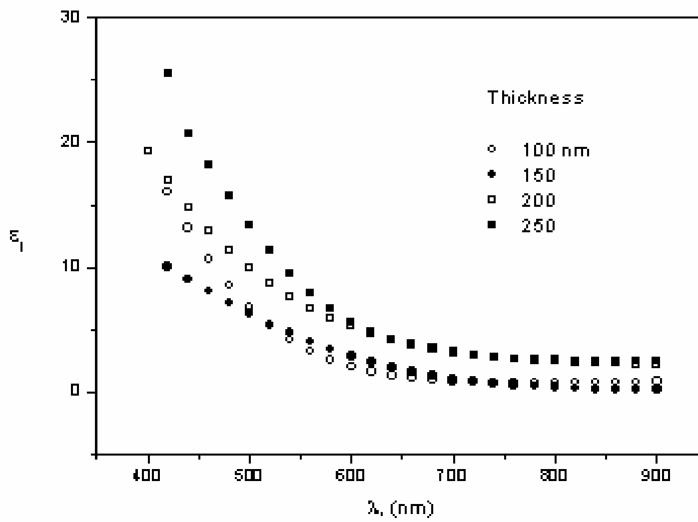

Fig. (7): The relation between the imaginary part of the dielectric constant (ε_i) and the wavelength for $Ge_{30}Se_{50}Te_{20}$ films.

The knowledge of the real and imaginary parts of the dielectric constant provides information about the dissipation factor which is the ratio of the imaginary part of the dielectric constant to the real part, and is given by [34]:

$$\tan\delta = \frac{\varepsilon_i}{\varepsilon_r} \qquad (13)$$

i.e. the larger the imaginary part of the dielectric constant or the smaller the real part of the dielectric constant, the larger is the dissipation factor.

The dissipation factor was calculated and plotted in Fig. (8) as a function of frequency for different film thickness. As seen from Fig., the dissipation factor decreased over the whole frequency range with increase in film thickness from 100 to 200 nm. For the 250 nm thickness sample, an increase was first shown more than thinner samples till frequency 4.2E+14 Hz, than it followed the normal trend.

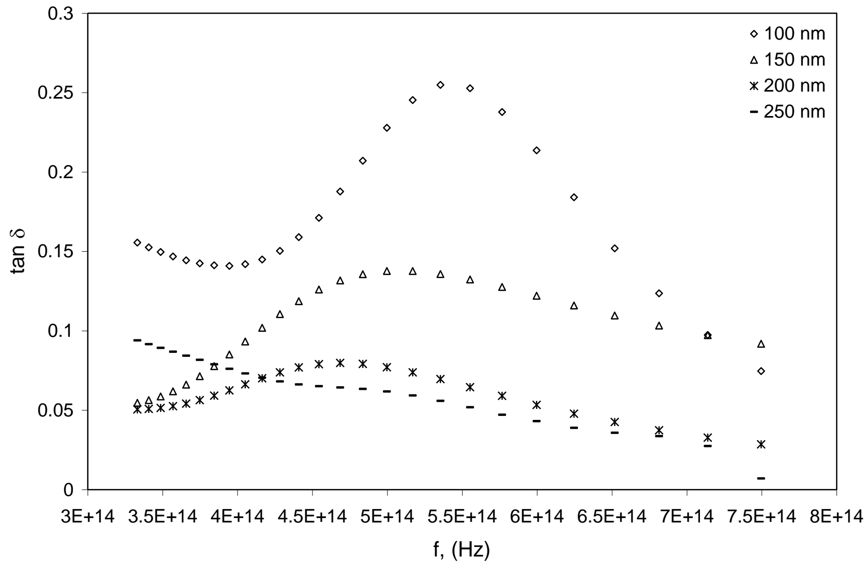

Fig (8): Dependence of the dissipation factor on the photon frequency for different film thickness

The real component of the dielectric constant could be approximated by the following equation [35]:

$$\varepsilon' = n^2 = \varepsilon_\infty - \left(\frac{e^2}{\pi c^2}\right)\left(\frac{N}{m^*}\right)\lambda^2 \quad \text{...............(14)}$$

where e is the electronic charge, c the velocity of light and (N/m^*) the ratio of the carrier concentration (N) to the effective mass (m^*). From eq. (14), plotting n^2 versus λ^2, the high-frequency dielectric constant (ε_∞) and the carrier concentration (N/m^*) could be determined, as shown in Fig. (9). The calculated values of ε_∞ and N/m^* for the films are given in table 1. The table shows that

the values of the high dielectric constant increases with increasing the film thickness up to 200 nm, which agrees with previously published data on different chalcogenide compounds [15, 27]. This increase was attributed to the increase in saturation of the dangling bonds [15] and due to change in the internal microstructure induced by the film thickness [27]. The results shown in Table (1) show the carrier concentration decreased with increase in film thickness.

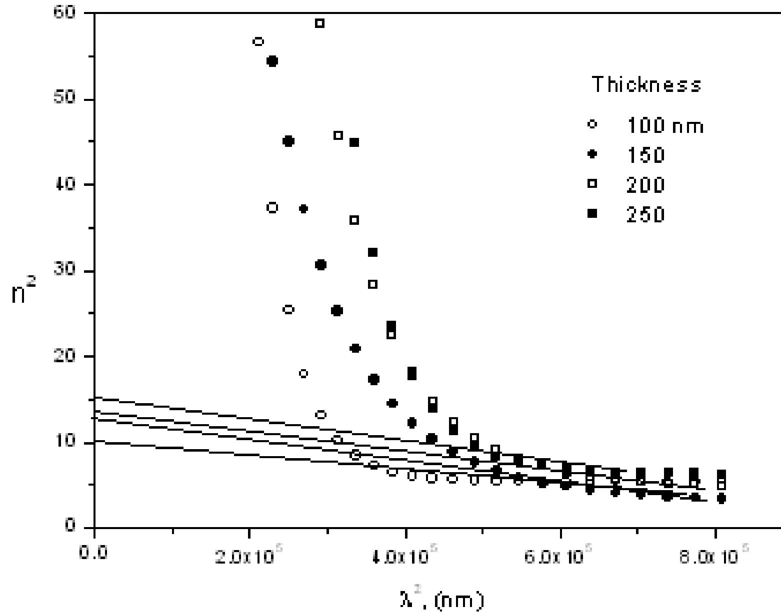

Fig. (9): The relation between the relative permittivity ($\varepsilon' = n^2$) and the square of wavelength (λ^2) for $Ge_{50-x}Se_{50}Te_x$ films.

The high frequency properties of $Ge_{30}Se_{50}Te_{20}$ films could be treated as a single oscillator. According to the single-effective oscillator model proposed by Wemple and DiDomenico, the optical data could be described to an excellent approximation by the following relation [36]:

$$\frac{1}{n^2 - 1} = \frac{E_w}{E_d} - \frac{(h\nu)^2}{E_w E_d} \quad \text{.............................(15)}$$

where n is the refractive index, E_w is the single oscillator energy, also called the average energy gap and E_d is the dispersion energy, which is a measure of the average strength of the interband optical transition.

Plotting $(n^2-1)^{-1}$ against $(h\nu)^2$, shown in Fig. (10), determines the oscillator parameters. The values of E_w and E_d can be directly determined from the slope $(E_wE_d)^{-1}$ and the intercept on the vertical axis (E_w/E_d). The calculated values of E_w and E_d are shown in table 1. It could be concluded from table 1 that E_w decreased with increasing film thickness from 100 to 200 nm, then it increased, showing the same trend as that of the optical gap E_g.

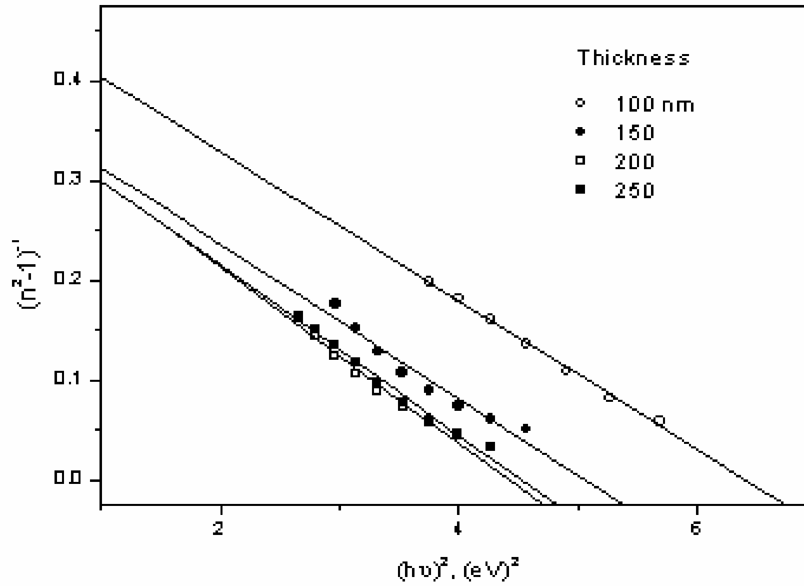

Fig. (10): $(n^2-1)^{-1}$ vs. the square of the photon energy $(h\nu)^2$ for $Ge_{30}Se_{50}Te_{20}$ films.

The obtained data of the refractive index can be also analyzed to yield the oscillator wavelength (λ_o) and the average oscillator strength (S_o) using the Sellmeier's dispersion formula [37] :

$$\frac{1}{n^2-1} = \frac{1}{S_o\lambda_o^2} - \left(\frac{1}{S_o}\right)\frac{1}{\lambda^2} \quad \text{.......................(16)}$$

The relation between $(n^2-1)^{-1}$ and λ^{-2} of $Ge_{30}Se_{50}Te_{20}$ films at different thickness is shown in Fig. (11). The oscillator wavelength (λ_o) and the average oscillator strength (S_o) are calculated from the slope and the intersection of the straight lines in Fig (11). The values of λ_o and S_o are listed in Table (1). It can

be seen from the table that values of the oscillator strength (S_o) and oscillator wavelength (λ_o) increase with increasing the film thickness. Similar conclusion for S_o was reported on a study on AsSeGe amorphous films [19].

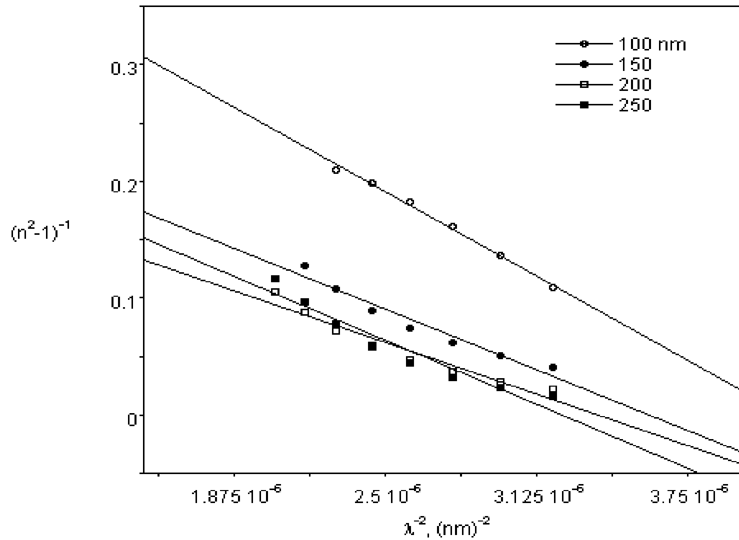

Fig. (11): $(n^2-1)^{-1}$ vs. λ^{-2} for different thickness$Ge_{30}Se_{50}Te_{20}$ films.

The optical response of a material is most conveniently studied in terms of the optical conductivity. It could be calculated using the absorption coefficient from the following relation [38]:

$$\sigma = \alpha nc / 4\pi \qquad (17)$$

where c is the velocity of light. The variation of □ with *h*□ for different film thickness is shown in Fig. (12) From Fig., a decrease in the optical conductivity is realized with increasing the thickness from 100 to 200 nm. Then, an increase in optical conductivity happens for the 250 nm film thickness.

The above calculated variations in the optical properties could be interpreted on the basis of the local field correction [39]. With the increase in film thickness, a denser optical medium is created and the individual atomic dipoles respond to the local field that they experience. Therefore, the actual local electric field experienced by a dipole takes the form:

$$E_{local} = E + E_{otherdipoles} \qquad (18)$$

where E and $E_{other\ dipoles}$ represents the field due to the external field and the other dipoles respectively. According to Lorentz, the increase in $E_{other\ dipoles}$ has an impact on the resultant polarization of the medium (P) increasing its value, according to the following relation:

$$P = N\varepsilon_o \chi_a E_{local} \qquad (19)$$

where N is the number of atoms per unit volume, ε_o the permittivity of vacuum and χ_a is the electric susceptibility. Such an increase in the micro polarization may explain the increase in the calculated values of the refractive index and dielectric constants with increasing the film thickness.

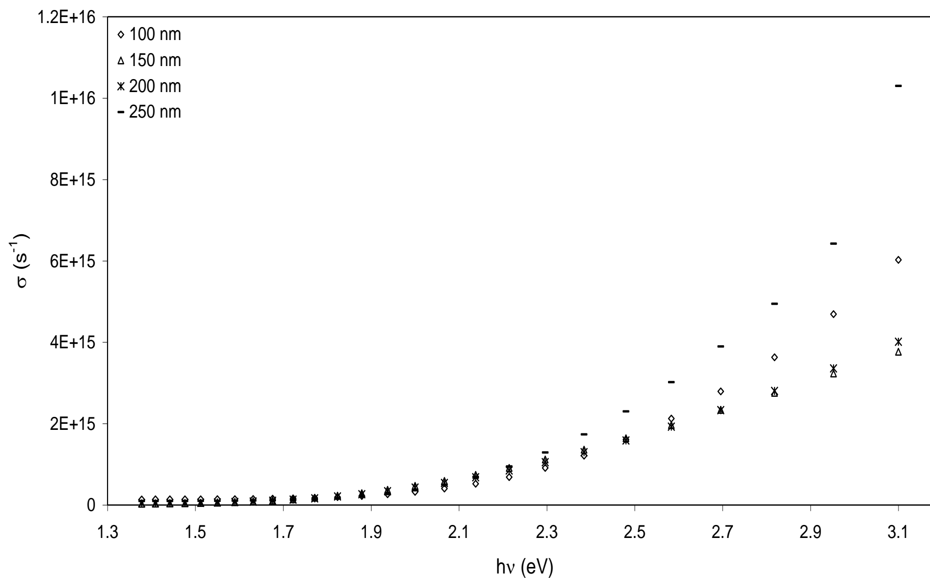

Fig. (12): Plot of optical conductivity σ versus $h\nu$ for different thickness $Ge_{30}Se_{50}Te_{20}$ films.

In case of the 250 nm thickness film, a kind of saturation is found for the effect of the local field correction. Greater deposition builds up a more homogeneous network minimizing the number of defects by saturating the dangling bonds and decreasing the density of localized states located in the band gap. This results in increasing the optical band gap and decreasing the value of the Urbach parameter.

4. Conclusions:

The relatively simple and straightforward method which has been proposed by Swanepoel [12], was used for determining the optical constants of $Ge_{30}Se_{50}Te_{20}$ chalcogenide films using only the transmission spectra. This method is based on the upper and lower envelopes of normal-incidence optical transmission spectra.

The optical constants n, ε_r, ε_i and ε_∞ increased with thickness in the range 100 -200 nm. This behavior was interpreted on the basis of the local field correction.

The optical band gap of $Ge_{30}Se_{50}Te_{20}$ chalcogenide films exhibits allowed indirect and direct transitions. The values of direct and indirect energy gap decrease with increasing the film thickness from 100 to 200 nm. For the 250 nm thickness, the band gap increased which is attributed to the saturation of dangling bonds for thicker films.

The oscillator energy E_w and the oscillator strength E_d or dispersion energy depend on the film thickness.

The oscillator wavelength (λ_o) and the average oscillator strength (S_o) increase with increasing the film thickness.

The dissipation factor decreases with increase in film thickness and optical conductivity decreased in the range 100 -200 nm and then increases for thicker films

References:

1. R Mehra, M R Kumar and P C Mathur, *Thin Solid Films,* **17**, 15 (1989).
2. J Nishi, S Morimoto, I Ingawa, R Iizuka, T Yamashita, *J Non-Cryst Solids*, **140**, 199 (1992).
3. J A Savage, *Infrared Optical Materials and their Antireflection Coatings*, Adam Hilger, Bristol, (1985).
4. H Nasu and J D Mackenzie, *Opt Eng*, **26**, 102 (1987).
5. W Leung, N W Cheung and A R Neuruther, *Appl Phys Lett*, **46**, 481 (1985).
6. J Feinleib, J P De Neufville, S C Moss and S R Ovshinsky, *Appl Phys Lett*, **18**, 254 (1971).
7. D Adler, *Sci Amer*, **236**, 36 (1977).
8. S R Ovshinsky, *phys. Rev Lett*, **21**, 1450 (1968).
9. R Zallen, *The physics of amorphous Solids*, (Willey, New York, 1983).
10. P Sharma and S C Katyal, *J Phys D:Appl Phys*, **40** 2115 (2007).
11. P Sharma and S C Katyal, *Thin Solid Films,* **515**, 7966 (2007).
12. R Swanepoel, *J Phys E: Sci Instrum*, **16**, 1214 (1983).
13. P Sharma and S C Katyal, *Mat Lett*, **61**, 4516 (2007).
14. S Velumani, X, P Mathew, J Sebastian, Sa K Narayandass and D Mangalaraj, *Sol. Energy mat. and Sol. Cells*, **76**, 347 (2003).
15. A A Abu-Sehly and M. Abd-Elrahman, *J Phys and Chem Solids,* **63**, 163 (2002).
16. D. P. Padiyan, A. Marikani and K. R. Murali, *Mat. Chem and Phys*, **78**, 51 (2002).
17. D. P. Padiyan, A. Marikani and K. R. Murali, *Mat. Chem and Phys*, **88**, 250 (2004).
18. D. P. Padiyan, A. Marikani and K. R. Murali, *Alloys and Compounds*, **365**, 8 (2004).
19. S. M. El-Sayed and G. A. M. Amin, *Vacuum*, **62**, 353 (2001).
20. J. P. Enriquez and X. Mathew, *Sol. Energy Mat. and Sol. Cells*, **76**, 313 (2003).
21. S. Agilan, D. Mangalaraj, Sa. K. Narayandass and G. M. Rao, *Physica B*, **365**, 93 (2005).
22. U. P. Khairnar, D. S. Bhavsar, R. U. Vaidya and G. P. Bhavsar, *Mat. Chem. and Phys*., **80**, 421 (2003).
23. S. K. Biswas, S. Chaudhuri and A. Chaudhuri, *Phys. Stat. Sol. (a)*, **105**, 467 (1988).
24. M. A. Abdel-Rahim, *J Phys and Chem Solids*, **60**, 29 (1999).
25. E. Abd El-Wahabb, M. M. El-Samanoudy and M. Fadel, *Appl. Surf. Sci*, **174**, 106 (2001).
26. Y. H. Liu, L. Meng and L. Zhang, *Thin Sol. Films*, **479**, 83 (2005).

7. M. I. Abd-ElRahman, A. A. Abu-Sehly and A. S. Soltan, *phys stat. sol. (a),* **191**, 169 (2002).

28. A. Abd El-Rahman, A. M. Eid, M. Sanad and R. M. El-Ocker, *J. Phys. Chem. Solids*, **59**, 825 (1998).

29. J Tauc, *Amorphous and liquid Semiconductors*, Ed. J. Tauc, Plenum, New York, Ch. 4, (1974).

30. E.A. Davis and N. F. Mott, *Phil. Mag*., **22**, 903 (1970).

31. F. Urbach, *Phys Rev*; **92**, 1324 (1953).

32. J Tauc, *The Optical Properties of Solids*, Amsterdam, North-Holland, (1970).

33. M. Fox, *Optical Properties of Solids*, Oxford, University Press, p. 6 (2001).

34. F. Yakuphanoglu, A. Cukurovali and I. Yilmaz, *Physica B*, **351**, 53 (2004).

35. E KH Shoker and M M Wakkad, *J. Mater Sci*, **27**, 1197 (1992).

36. S. H. Wemple, M. DiDominico, *Phys. Rev. B*, **3**, 1338 (1971).

37. D T F Marple. *J Appl Phys,* **35**, 539 (1964).

38. J. I. Pankove, *Optical Processes in Semiconductors,* New York, Dover, p. 91 (1975).

39. M. Fox, *Optical Properties of Solids*, Oxford, University Press, p. 39 (2001).